BGV beam-gas collisions at IR4 and related radiation levels

Daniel Prelipcean[1,2] (daniel.prelipcean@cern.ch), Giuseppe Lerner[1], Rubén García Alía[1], Bernadette Kolbinger[1], Helene Guerin[1], James Storey[1], Alessio Galloro[1], Roberto Kersevan[1]

[1]CERN (CH-1211 Geneva), [2]Technical University of Munich (DE-80333 München)

1. The Large Hadron Collider

The radiation levels caused by the Beam Gas Vertex (BGV) [1] operation in Interaction Region 4 (IR4) of the Large Hadron Collider (LHC) [2] at CERN are discussed. The key ingredients of the analysis are:

- Measurements of Total Ionising Dose (TID) performed with the Beam Loss Monitoring (BLM) system [3] from LHC Run 2 (2015-2018), during the operation of the BGV demonstrator.
- FLUKA [4-6] simulations of beam gas interactions for the past LHC Run 2 (benchmark) and future HL-LHC scenarios (radiation levels prediction).

Main goal is to determine whether the operation of these devices can lead to Radiation to Electronics (R2E) [7-8] issues, or excessive heat loads on cryogenics systems.

2. Radiation source and normalization

Any residual gas will lead to beam-gas interactions causing local radiation showers. This effect can be used to measure the beam profile/position, if there are sufficient secondaries produced. The Beam Gas elements in IR4 inject gas (typically Ne) to increase the local density and measure the secondaries for beam profile reconstruction. The radiation levels scale as:

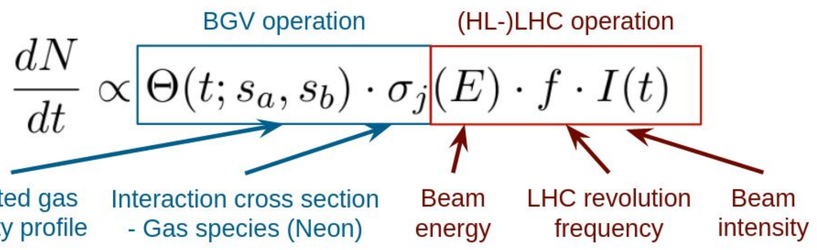

with the number of charges I (t) passing through the gas, the LHC revolution frequency f = 11 245 Hz, the inelastic cross section estimated [9] at $\sigma_{p+Ne,inel}$ = 320 mb, for a beam of 6.5 or 7 TeV protons hitting the gas atoms (assumed at rest, as their thermal energy of 0.025 eV at room temperature is negligible), and the gas with an integrated density profile $\Theta(t; s_a, s_b)$ along s-coordinate in the accelerator region $[s_a, s_b]$ as

$$\Theta(t; s_a, s_b) = \rho_{max} \cdot \int_{s_a}^{s_b} \frac{\rho(s)}{\rho_{max}} ds$$

where $\varrho(s)$ is the number density of gas atoms and ϱ_{max} is the peak value of the profile. From a measurement perspective, just one data point is available at the BGV via a pressure gauge located at the assumed peak ϱ_{max}, but no measured information on the distribution width. Nevertheless, the gas density profile used in FLUKA (see the lower pannel of Fig. 4) has been simulated using MOLFLOW+ [10].

6. Conclusions

The main results of this study are the observed proportionality between the TID measured by the BLMs and the product of pressure and intensity up to half-cell 9 included, signaling that in this portion of tunnel the BGV was indeed the main radiation source. The comparison between the Run 2 measurements and the FLUKA simulation reveals a good agreement, which is a further confirmation that we understand the origin of the radiation levels. From a machine protection point of view, the simulated radiation levels are not an issue for what concerns the heat loads on the magnets, both as maximum power density or as total power dissipated on the entire magnet. Similarly, the TID levels do not rise any concerns in terms of cumulated damage to the magnets. A similar study is expected for the Beam Gas Curtain (BGC) monitor and its Run 3 operation.

3. Measured BLM data from the LHC Run 2

During a fill, when gas is injected in the BGV, one expects the BLM TID rate signal to be proportional to the product of pressure and intensity. For the analysis, we have identified time periods (up to ~1h), with rather constant gas pressure, and higher than a predefined threshold of 2×10^{-8} mbar.

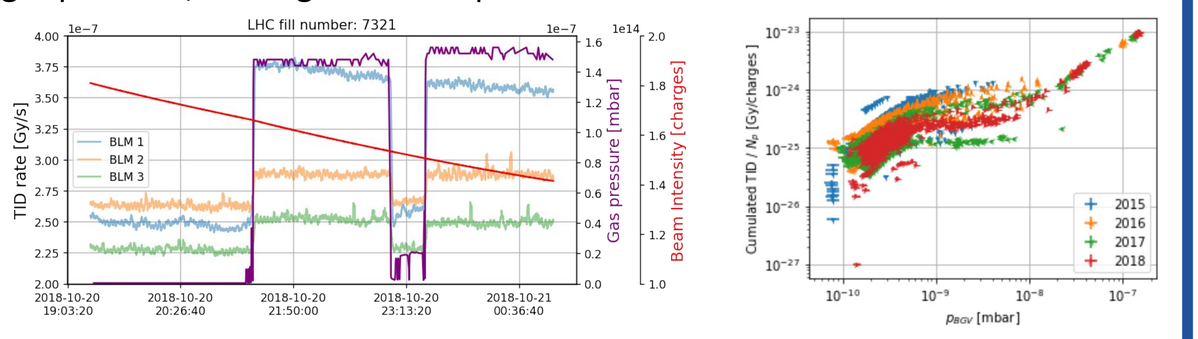

Fig. 2: (Left) The measured TID rate for the first three BLMs downstream of the BGV within a time period of LHC fill number 7321, showing the beam intensity Np as measured by the BCT instruments for beam 2 and the BGV pressure gauge reading p_{BGV}. (Right) The measured TID of BLM 1 (the most irradiated during Run 2) divided by the number of protons passing through the BGV N_p plotted against the average BGV pressure gauge reading p_{BGV} for all the time periods under consideration, for each year of Run 2 operation.

4. FLUKA simulation

The radiation source consisted in just the inelastic beam-gas interactions, as the position of the interactions is sampled along a Continuous Distribution Function (CDF) function given by the gas density profile in the tunnel, and the interaction secondaries are propagated in the LHC tunnel geometry model.

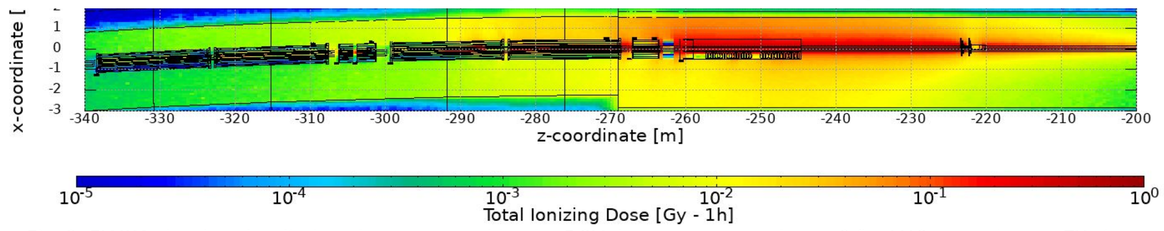

Fig. 3: FLUKA simulated radiation shower caused by the BGV demonstrator on beam 2 for LHC operation, as ZX view, displaying how the shower extends over several tens of meters. The TID is provided at beam height, for a beam at E = 6.5 TeV with an intensity of $N_i = 3 \cdot 10^{14}$ charges, and normalized for 1 operational hour, for a gas pressure profile peaked at $0.73 \cdot 10^{-7}$ mbar, corresponding to the averaged measured maxima.

5. FLUKA vs Measured data and HL-LHC levels

The shape of the BLM TID profile is well reproduced with a good global agreement within a factor of 2 between simulations and measurements, with just one outlier. Additionally, HL-LHC predictions are made solely on FLUKA simulations. Moreover, the BGV was the main contributor for integrated yearly radiation levels in cell 7 and for selected BLMs in the next two cells downstream. The analysis shown here stops at -360 m from the center of IR4 (or 150 m downstream of the BGV on beam 2), because the measured radiation levels induced so far away fall below other sources of radiation.

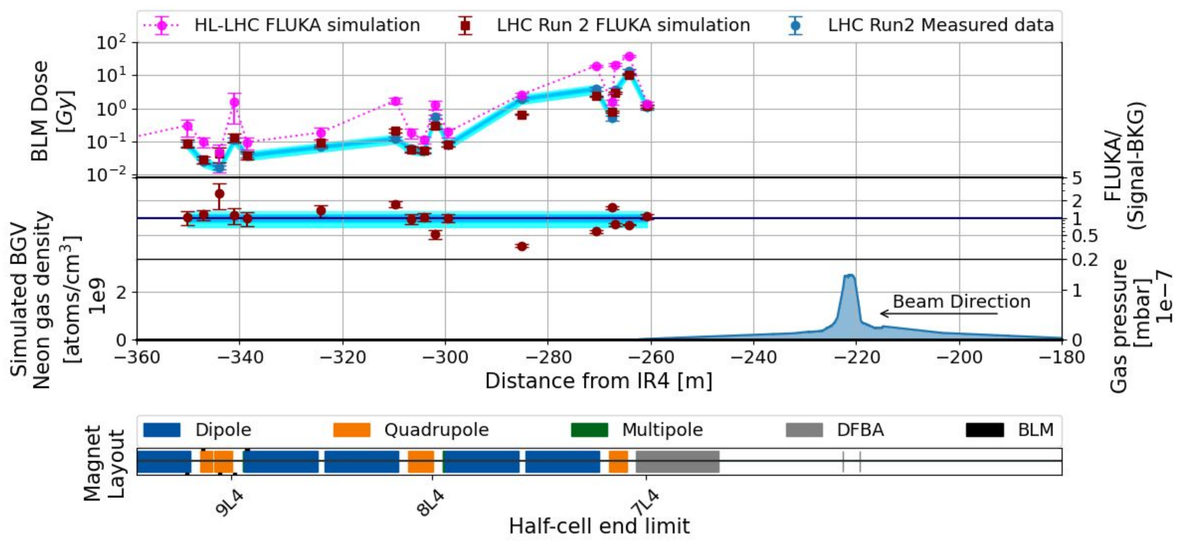

Fig. 4: Top panel: BLM pattern downstream the BGV placed on beam 2 as measured over the Run 2 proton runs (blue points) and as simulated by FLUKA for LHC (red points) for 170 h of operation and HL-LHC (magenta points) for 400 h of operation. Mid panel: Ratio between simulation values and measured data for Run 2. Lower panel: BGV gas density profile. Bottom pad: The machine layout and the BLM locations, where we assumed that the BLMs during HL-LHC operation will be in the same position as in Run 2.

References

1. The BGV Collaboration , Noninvasive LHC transverse beam size measurement using inelastic beam-gas interactions. Physical Review Accelerator Beams, vol. 22, issue 4, April 2019. https://link.aps.org/doi/10.1103/PhysRevAccelBeams.22.042801.
2. O. Brüning et al. LHC Design Report. CERN Yellow Reports: Monographs. CERN, Geneva, 2004. doi:10.5170/CERN-2004-003-V-1. URL https://cds.cern.ch/record/782076.
3. E. B. Holzer et al. Beam loss monitoring system for the LHC. IEEE Nuclear Science Symposium, 2:1052 –1056, November 2005. doi: 10.1109/NSSMIC.2005.1596433.
4. FLUKA website. URL https://fluka.cern.
5. C. Ahdida et al. New Capabilities of the FLUKA Multi-Purpose Code. Frontiers in Physics, 9, 2022. ISSN 2296-424X. URL https://www.frontiersin.org/article/10.3389/fphy.2021.788253.
6. G. Battistoni et al. Overview of the FLUKA code. Annals Nucl. Energy, 82:10–18, 2015. doi: 10.1016/j.anucene.2014.11.007.
7. The Radiation to Electronics (R2E) project at CERN, website. URL https://r2e.web.cern.ch/.
8. M. Brugger. R2E and availability. In Proc. of Workshop on LHC Performance, Chamonix, France, 2014.
9. M. Ferro-Luzzi. Beam-gas interactions, 2020. URL: https://arxiv.org/abs/2006.06490.
10. R. Kersevan and M. Ady. Recent Developments of Monte-Carlo Codes Molflow+ and Synrad+. volume IPAC2019, pages 1327–1330, Geneva, Switzerland, Jun. 2019. JACoW Publishing. doi: doi:10.18429/JACoW-IPAC2019-TUPMP037.